Cancer Cell
Article

Bone Marrow-Derived Myofibroblasts Contribute to the Mesenchymal Stem Cell Niche and Promote Tumor Growth

Michael Quante,[1,6] Shui Ping Tu,[1,5,6] Hiroyuki Tomita,[1] Tamas Gonda,[1,2] Sophie S.W. Wang,[1] Shigeo Takashi,[1] Gwang Ho Baik,[1] Wataru Shibata,[1] Bethany DiPrete,[1] Kelly S. Betz,[1] Richard Friedman,[3] Andrea Varro,[4] Benjamin Tycko,[2] and Timothy C. Wang[1,*]
[1]Division of Digestive and Liver Diseases
[2]Institute for Cancer Genetics and Department of Pathology
[3]Department of Biomedical Informatics
Columbia University, New York, NY 10025, USA
[4]Department of Physiological Laboratory, School of Biomedical Sciences, University of Liverpool, Liverpool L69 3BX, UK
[5]Susan L. Cullman Laboratory for Cancer Research, Department of Chemical Biology, Center for Cancer Prevention Research, Ernest Mario School of Pharmacy, Rutgers, The State University of New Jersey, Piscataway, NJ 08854, USA
[6]These authors contributed equally to this work
*Correspondence: tcw21@columbia.edu
DOI 10.1016/j.ccr.2011.01.020

SUMMARY

Carcinoma-associated fibroblasts (CAFs) that express α-smooth muscle actin (αSMA) contribute to cancer progression, but their precise origin and role are unclear. Using mouse models of inflammation-induced gastric cancer, we show that at least 20% of CAFs originate from bone marrow (BM) and derive from mesenchymal stem cells (MSCs). αSMA+ myofibroblasts (MFs) are niche cells normally present in BM and increase markedly during cancer progression. MSC-derived CAFs that are recruited to the dysplastic stomach express IL-6, Wnt5α and BMP4, show DNA hypomethylation, and promote tumor growth. Moreover, CAFs are generated from MSCs and are recruited to the tumor in a TGF-β- and SDF-1α-dependent manner. Therefore, carcinogenesis involves expansion and relocation of BM-niche cells to the tumor to create a niche to sustain cancer progression.

INTRODUCTION

Tumors consist of cancer cells and diverse stromal cells that constitute the tumor microenvironment and contribute to tumor progression. Stem cells or their immediate progeny can give rise to various tumor-contributing cells through a dysregulated self-renewal process (Wicha et al., 2006), but the origin of many niche cells critical for tumor growth (Li and Neaves, 2006) has not been established. Much of the tumor stroma consists of cancer-associated fibroblasts (CAFs) that express α-smooth muscle actin (αSMA). CAFs closely resemble myofibroblasts (MFs) that are present in the gastrointestinal mucosa. Clinical evidence supports the contribution of stroma to the development of a variety of tumors (Coussens and Werb, 2002). In general there is a higher incidence of tumor formation in tissues with chronically inflamed stroma, particularly *Helicobacter pylori* gastritis, which is associated with gastric cancer (Houghton and Wang, 2005).

Phenotypically, CAFs resemble normal gastrointestinal MFs in that they express αSMA and other MF markers such as vimentin or FSP1; biologically they are different, and it remains puzzling why CAFs would appear only in the setting of cancer, but not in the normal adult organs. Tumors that have a desmoplastic stroma, consisting of more stromal cells disrupting the tissue

Significance

Tumorigenesis is driven by alterations in tumor cells but also changes in the stromal microenvironment. We demonstrate that a significant percentage of CAFs in inflammation-associated gastric cancer originates from MSCs and that MFs contribute to the normal stem cell niche in the BM. MSCs give rise to their own niche cells, which might apply to other stem cell niches. In inflammation-induced cancer progression, MFs increase in the BM niche and blood during progression to dysplasia. Therefore, we propose a model in which the earliest stages of tumor development are characterized by remodeling of the BM, followed by relocation of the MSC-CAF stem cell niche to the tumor site where it promotes tumor progression.

homogeneity, often have a poorer prognosis (Maeshima et al., 2002). CAFs isolated from breast cancer tissue promote proliferation of cancer cell lines, increase angiogenesis to a greater extent, and have a distinct gene expression pattern compared to normal fibroblasts (Allinen et al., 2004). CAFs isolated from prostate cancer direct tumor progression of initiated prostatic epithelium and can transform nontumorigenic human prostatic epithelial cell lines into tumorigenic ones (Hayward et al., 2001). CAFs express increased levels of the chemokine SDF-1 (Orimo et al., 2005) and genes such as *Gremlin-1* that are not expressed in most normal tissues (Sneddon et al., 2006). Finally, we recently showed that CAFs were more hypomethylated than normal gastric stromal cells (Jiang et al., 2008).

CAFs have altered biology compared to normal MFs and seem to accumulate in tumors. A number of studies have explored the origins of CAFs, which include resident fibroblasts (Orimo et al., 2005), smooth muscle cells, endothelial cells, epithelial cells (through EMT), fibrocytes, and bone marrow (BM)-derived cells such as mesenchymal stem cells (MSCs) (Direkze et al., 2003; Karnoub et al., 2007). Chronic inflammation associated with increased cancer risk (Forbes et al., 2004) and tumor xenografts (Ishii et al., 2003) recruit BM-derived MFs. In gastric tumors of patients that received gender-mismatched BM transplants (BMTs), many CAFs are bone marrow derived (Worthley et al., 2009). However, the precise BM cell type that gives rise to CAFs remains unclear.

Several studies have pointed to MSCs as a potential source of CAFs (Guo et al., 2008). MSCs, when mixed with weakly metastatic human breast carcinoma cells, increase the metastatic abilities of cancer cells (Karnoub et al., 2007). MSCs exposed to tumor-conditioned medium assume a CAF-like phenotype, including sustained expression of SDF-1 and the ability to promote tumor cell growth (Mishra et al., 2008). MSCs are defined as pluripotent stem cells that contribute to normal bone, adipose, cartilage, and muscle (Pittenger et al., 1999). MSCs originate in the BM but can be found throughout the body; they are often involved in tissue remodeling after injury or chronic inflammation. BM-derived cells (BMDCs) are often recruited to carcinogenic sites by cytokines such as IL-1β (Houghton et al., 2004; Tu et al., 2008), and indeed, CAFs promote further cell recruitment through secretion of chemokines such as SDF-1 (Orimo et al., 2005). MSCs are among the BMDCs that have been shown to be recruited to tumors and to promote their growth. Although some studies have suggested that MSCs can differentiate into CAFs, the differentiation of MSCs into CAFs or MFs has, to our knowledge, not been demonstrated conclusively (Stappenbeck and Miyoshi, 2009). In this study we aimed to investigate the cellular origin and role of CAFs within the BM and analyzed their function in normal BM and in the tumor microenvironment.

RESULTS

αSMA+ MFs Increase with Gastric Dysplasia and Contribute to a Desmoplastic Tumor Microenvironment

To understand the changes that occur in stromal cells during gastric cancer progression, we analyzed αSMA-RFP transgenic mice that express RFP under the direction of the αSMA promoter and collagen-α1-EGFP transgenic mice that express EGFP under the control of the collagen-α1 promoter (Magness et al., 2004). A tissue-specific expression pattern for the 3 kb αSMA promoter fragment-driven RFP relative to endogenous αSMA expression was confirmed in gastric mucosa (Figure 1D; see Figure S1A available online). Both sets of mice were infected with *Helicobacter felis* (*H. felis*), resulting in chronic gastritis, atrophy, metaplasia, and dysplasia (Figure S1B). In uninfected mice, few αSMA-RFP+ MFs were present in gastric tissue, whereas collagen-α1/EGFP+ stromal cells were abundant (Figures 1A and 1B). Twelve to 18 months after infection, collagen-α1/EGFP+ fibroblasts and αSMA-RFP+ fibroblasts increased with chronic inflammation and cancer progression (Figures 1A–1C). Although collagen-α1-EGFP+ fibroblasts were abundant at early, they increased only slightly at late stages of neoplasia; αSMA-RFP+ fibroblasts were scarce early after infection but increased markedly at later stages, particularly during dysplasia, suggesting that αSMA-RFP+ fibroblasts contribute to the neoplastic process. They were defined as MFs by their expression of endogenous αSMA and vimentin (data not shown). Similarly, αSMA/collagen-α1 double-positive cells increased with dysplasia (Figures S1C and S1D), especially in invasive or highly dysplastic regions (Figure S1E). Additionally, we crossed the αSMA-RFP mice with IL-1β/αSMA-RFP mice, which express human IL-1β specifically in the stomach and develop spontaneous gastric inflammation and cancer (Tu et al., 2008). The expression of αSMA and RFP increased by 6 and 12 months in IL-1β/αSMA-RFP mice (Figure 1D).

We isolated fibroblastic cells from stomachs of αSMA-RFP mice and specifically cultured the MFs using glutamine withdrawal (McKaig et al., 1999) (Figure S1F). Sorting after four population doublings (PDs) revealed that 33% of the cells from uninfected WT mice and 70% from mice with dysplasia expressed RFP (Figure 1E), suggesting that αSMA/RFP+ CAFs have a growth advantage over αSMA/RFP− WT MFs, correlating with in vivo results. Gastric RFP+ MFs of uninfected mice grew for up to 25 PDs. In contrast, gastric RFP+ CAFs from long-term *H. felis*-infected mice grew much faster and up to 80 PDs. Interestingly, we observed that RFP+ cells, when cultured with sorted RFP− cells, appeared to be surrounded by RFP− cells (Figure S1G), suggesting the possibility that RFP+ cells might be providing a niche for RFP− cells. In addition, RFP+ CAFs isolated from long-term infected mice with dysplasia expressed increased amounts of TGF-β, IL-6, and TNF-α compared to WT RFP+ MFs (Figure S1H).

BMDCs Contribute to αSMA+ CAFs in an Inflammation-Related Model of Gastric Carcinogenesis

To determine how BMDCs contribute to stromal cells in an inflammation-dependent model of cancer, IL-1β mice were irradiated and transplanted with EGFP− (UBC-EGFP), RFP− (αSMA-RFP), or double-labeled (UBC-EGFP/αSMA-RFP) BM, and animals were observed for 12–14 months. Engraftment of MSCs was initially confirmed through isolation (Figure S2A) and characteristic differentiation (Figure S2B) of GFP+ MSCs isolated from BM 4 months after transplant, consistent with previously published studies (Wang et al., 2009), confirming that mouse BM MSCs can be transplanted (Simmons et al., 1987; Yokota et al., 2006). In vitro culture revealed that one-third of MSCs were GFP+ and, thus, donor derived (Figure S2A).

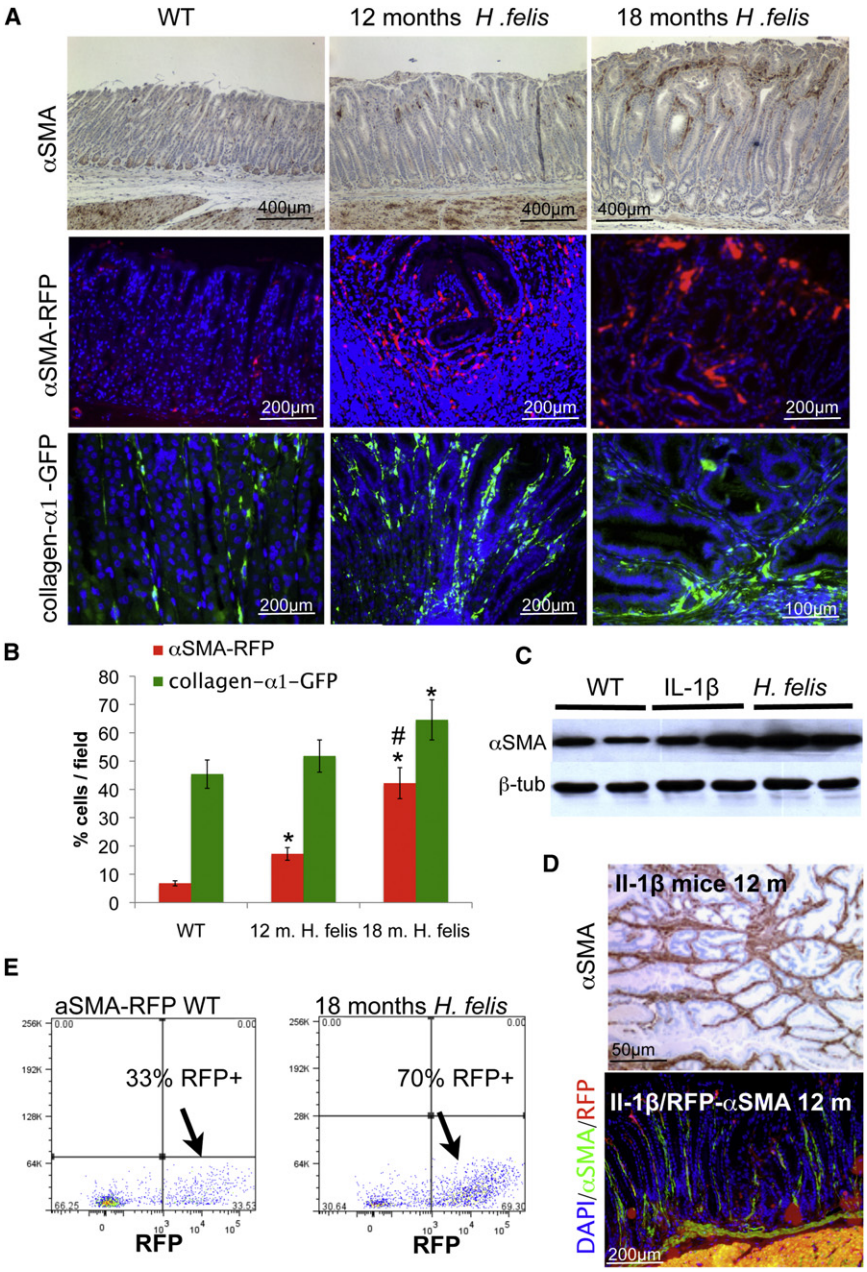

Figure 1. BM-Derived αSMA-Expressing Cells Contribute to the Tumor Microenvironment

(A) αSMA staining (upper panel) and endogenous αSMA-RFP (middle panel) or endogenous collgen-α1 (lower panel) expression in stomachs of αSMA-RFP/collagen-α1-GFP double-transgenic mice and following 12 or 18 months of *H. felis* infection.

(B) Relative number of αSMA (red) or collagen (green)-expressing cells in the stomach of αSMA-RFP/collagen-α1-GFP double-transgenic mice without and with 12 or 18 months of *H. felis* infection (*$p < 0.05$ compared to WT and #$p < 0.05$ compared to 12 months).

(C) Western blot for αSMA and β-tubulin in gastric tissue of WT, IL-1β transgenic mice, and WT mice with 18 months of *H. felis* infection.

(D) αSMA staining in a dysplastic region in 12-month-old IL-1β transgenic mice and 95% colocalization of endogenous RFP expression and αSMA in stomachs of 12-month-old IL-1β/αSMA-RFP mice.

(E) FACS analysis of RFP+ gastric MFs at eight PDs, isolated from uninfected αSMA-RFP mice (WT MFs) or *H. felis* (18 months)-infected αSMA-RFP mice (18-month *H. felis*).

All data are represented as mean ± SEM (see also Figure S1).

Transplantation of αSMA-RFP BM revealed abundant engraftment in the BM of RFP+ cells after 18 months (Figure S2C). In IL-1β or *H. felis*-infected mice that received labeled BM, the development of dysplasia was preceded by the influx of a large number of labeled cells (Figure 2A; Figure S2D). Although a large proportion of the EGFP+ cells were immune cells (e.g., lymphocytes and myeloid cells), 12 months after BMT in IL-β mice, and 18 months after BMT in *H. felis*-infected mice, approximately 20% of αSMA+ cells in regions of gastric dysplasia were EGFP+ (Figures 2A and 2C; Figure S2D), whereas few if any double-positive (αSMA+/EGFP+) cells were found in uninfected WT mice. To quantify the BMDCs, we transplanted BM from UBC-GFP/αSMA-RFP mice into WT *H. felis*-infected, IL-1β, or control mice. IHC and FACS revealed that in mice with dysplasia, 20% of the GFP+ BMDCs were also RFP+ (Figure 2B; Figure S2E). These findings point to a role for αSMA+/EGFP+ cells in inflammation-induced carcinogenesis.

We isolated and cultured MFs and CAFs from the stomachs of EGFP+ BM-transplanted 12-month-old WT and IL-1β mice to determine the contribution of BMDCs to the MF population (Figure S2F). After four PDs, more than 70% of CAFs from IL-1β mice (with dysplasia) were EGFP+, indicating their BM origin. Culture of RFP+/GFP+ CAFs (Figure 2F) from double-transgenic donors further confirmed that aSMA+ cells were BM derived. After sorting, the vast majority of EGFP− cells survived only a few PDs, whereas EGFP+ CAFs proliferated and could be cultured for at least 80 PDs and expressed MF markers (αSMA, vimentin), but not epithelial markers (E-cadherin; data not shown). No cells in the MF or CAF populations were positive for CD31, CD45, CD3e, CD11b, CD45R/B220, Ly6G, Ly-6C, or TER-119 based on FACS analysis (data not shown), indicating no contamination with leukocytes. BM-derived CAFs expressed significantly higher mRNA levels of TNF-α, IL-6, SDF-1, and TGF-1β (Figures S2G and S2H), compared to WT MFs.

These data suggest that a significant population of CAFs in the tumor microenvironment of inflammation-induced gastric cancer is BM derived and contributes to tumor promotion.

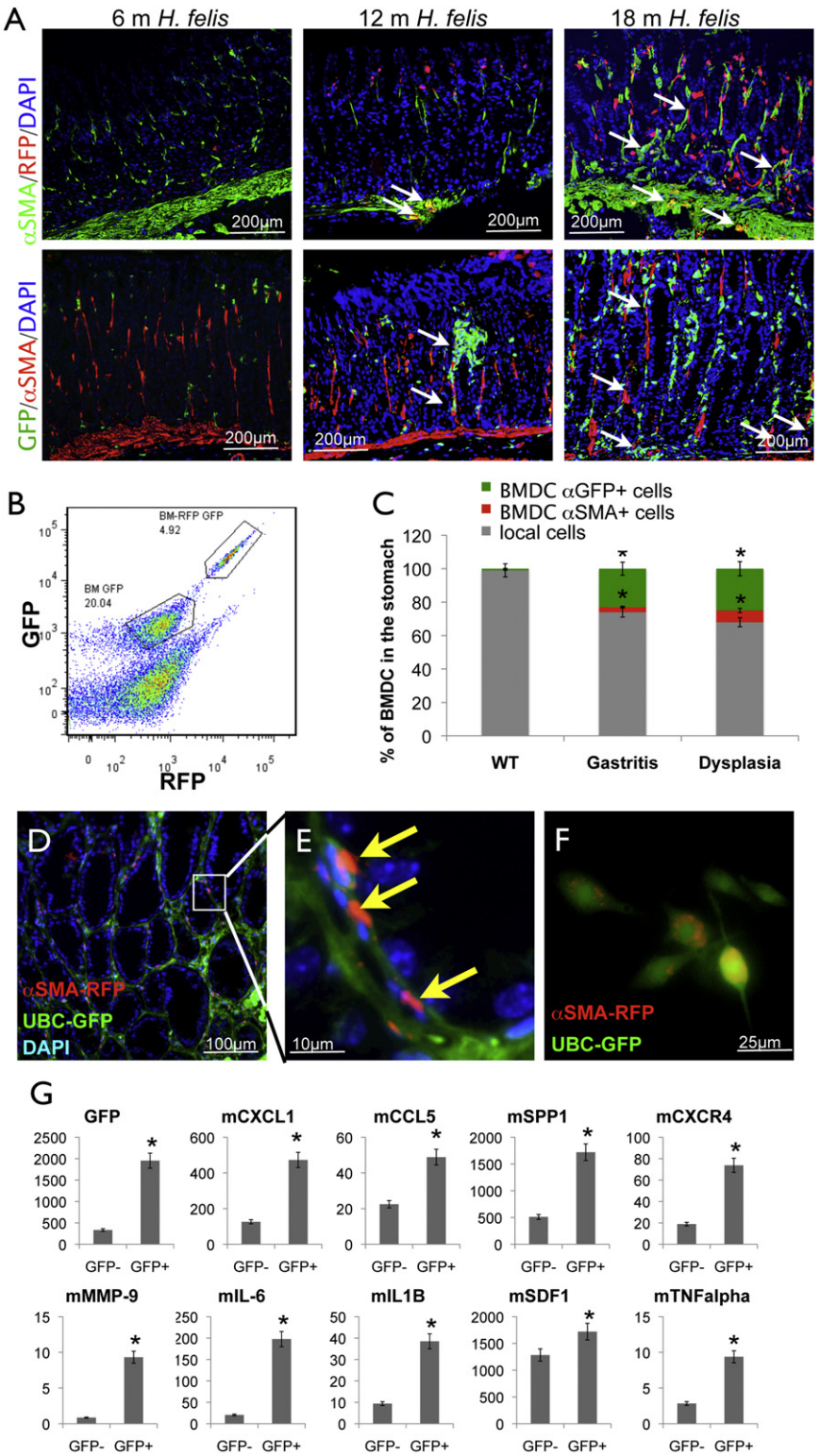

Figure 2. A Significant Portion of Gastric CAFs Originate from the BM

(A) GFP (lower panel) or RFP (upper panel) expression and costaining for αSMA and DAPI in stomachs of WT or 12 and 18-month-old mice with *H. felis* infection (arrows indicate αSMA and GFP or RFP coexpression) after UBC-GFP- or αSMA-RFP-labeled BMTs.

(B) FACS of freshly isolated gastric MFs from WT mice with double-labeled BMTs after 18 months of *H. felis* infection.

(C) FACS data on BM cell contribution to the tumor microenvironment in WT, IL-1β, and *H. felis*-infected WT mice harboring gastritis or dysplasia. Green, non-αSMA+ BMDCs; red, αSMA+ BMDCs; gray, all non-BMDCs (*$p < 0.05$).

(D and E) Endogenous RFP and GFP expression in stomach of 18-month-old *H. felis*-infected WT mice after UBC-GFP/αSMA-RFP− double-labeled BM transplantation.

(F) Endogenous RFP and GFP expression in in vitro culture of isolated MFs from stomachs of 18-month-old *H. felis*-infected WT mice after UBC-GFP/αSMA-RFP− double-labeled BM transplantation.

(G) Gene expression data after FACS of GFP(−) and GFP(+) CAFs from a BM-transplanted *H. felis*-infected IL-1β mouse. qRT-PCR for expression of GFP, CXCL1, CCL5, SSP1, CXCR4, MMP9, IL-6, IL-1β, SDF-1α, and TNFa (copies are calculated per 10,000 copies of GAPDH; *$p < 0.05$ compared to all other cells).

All data are represented as mean ± SEM (see also Figure S2 and Table S1).

Because resident CAFs could only be cultured for two to three passages and, thus, could not be used for extensive comparison to BM-derived CAFs, we additionally isolated total RFP(+) gastric CAFs (HF-CAF) from aSMA-RFP mice and compared them to GFP(+) BM-derived gastric CAFs (BM-CAFs). Only 20% of HF-CAFs were BM derived. We compared their gene expression directly after FACS (Figure S2I and Table S1). BM-CAFs expressed higher levels of inflammatory genes (IL-6, IL-1β, IL-33) and a number of tumor and stem cell-associated factors (CCL5, SPP1, Notch3, MMP9, CD47, CXCR4, PARP10) compared to HF-CAFs. To confirm that this gene expression signature represents the BM-derived fraction of the CAFs, we separated BM-transplanted GFP+ gastric CAFs from resident GFP− gastric CAFs from *H. felis*-infected IL-1β mice after short-term in vitro culture by FACS and analyzed their gene expression. BM-CAFs demonstrated an expression profile of selected inflammatory genes similar to what we observed using microarray (Figure 2G). We compared the gene expression signature of our BM-derived CAFs with a previously reported inflammatory gene signature for skin CAFs (Erez et al., 2010). Four out of the seven key inflammatory signature genes proposed by Erez et al. (2010) were also upregulated ($p < 0.05$) in our gene list (CXCL1, IL-1β, IL-6, SPP1) (Figure S2I and

Table S1). Additionally, we identified 20 out of 60 genes with a significant ($p < 0.05$) log fold change within the Erez gene list that were identically up or downregulated in our comparison of BM-CAFs versus HF-CAFs. These findings suggest the possibility that this inflammatory gene signature might be largely determined by the BM-derived CAFs.

Expansion of αSMA+ MFs in the BM of Mice with Gastric Dysplasia

To characterize the BM lineage that gives rise to αSMA+ CAFs, we screened BM from αSMA-RFP mice with and without *H. felis* infection and BM from αSMA-RFP/IL-1β mice for αSMA+ cells. FACS analyses showed rare αSMA-RFP+ cells in the BM of uninfected control mice (0.02% ± 0.007%) (Figure 3A; Table S2) but a significant stepwise increase in αSMA-RFP+ cells in the BM from aged IL-1β transgenic mice (1.2% ± 0.18%) and mice with long-term (18 months) *H. felis* infection (0.9% ± 0.1%), both with gastric dysplasia (Figure 3A), suggesting that long-term chronic inflammation and/or dysplasia is required for remodeling of the BM. In a model of accelerated gastric cancer (*H. felis* in combination with N-methyl-N-nitrosourea [MNU]; Tomita et al. [2010]), we confirmed the dependence of BM αSMA cell expansion on dysplasia (Figure 3A). Histopathological analysis confirmed a marked increase of RFP+ and αSMA+ cells in BM after 14 months of *H. felis* infection (Figure 3B). Although RFP+/αSMA+ cells were occasionally surrounded by small groups of CD34+ hematopoietic stem cells (Figure S3A), we could not confirm any significant correlation in the localization of these cell types. Whereas undetectable in uninfected control mice, we observed in the peripheral blood (0.009%) of mice with dysplasia rare RFP+ cells (Table S2), which expressed high levels of αSMA (Figure S3B). In addition the MSC and CAF cultures from dysplastic stomachs were morphologically very similar. Colony-forming units (CFUs) were consistently observed when we cultured gastric CAFs in MSC-specific media (Figure S3C). These data indicate that accumulation of differentiated αSMA+ BMDCs in the BM and blood correlates temporally with the development of gastric dysplasia.

MSCs are a possible source for MFs, so we established MSC cultures from whole BM from uninfected αSMA-RFP mice. The cultured, adherent cells were shown to be MSCs by their ability to form CFUs (Figure 3C) and differentiation into adipocytes and osteoblasts (Figures 3D and 3E). MSCs displayed longevity and grew exponentially for up to 80 days without signs of senescence or differentiation (Figure 4B) and with a normal karyotype (Figure S3D). Interestingly, MSC cultures also contained cells that expressed the RFP. Although histopathological evaluation showed a moderate number of αSMA/RFP+ cells in the BM, only 0.02% of fresh eluted whole BM expressed RFP by FACS, suggesting limitations to this extraction technique for stromal cells (Table S2). Nevertheless, 1.1% of cells after growth for several days in culture on plastic dishes and 50% or more of cells after several PDs expressed RFP (Table S2), indicating that myofibroblastic differentiation is highly favored under these in vitro conditions. IHC demonstrated that the RFP+ cells expressed high levels of endogenous αSMA, FSP1, and vimentin, but low levels of collagen (Figures 3F and 3G). These data confirm that murine BM-derived MSCs can differentiate into αSMA+ cells that resemble CAFs.

In the Heterogeneous MSC Population, αSMA(–) MSCs Give Rise to αSMA+ MFs that Function as Niche Cells

With continuous culture, MSCs contained a large proportion of αSMA-RFP+ cells, indicating the heterogeneous nature, similar to the BM-derived CAF population isolated from the stomach. FACS analysis of heterogeneous MSC cultures (Table S2) revealed that the majority of cells expressed RFP (71%) at six PDs but that this RFP+ population declined with more PD. When we compared the number of RFP+ cells after six PDs, we found significantly more RFP+ cells in MSCs derived from IL-1β/αSMA-RFP mice or *H. felis*-infected αSMA-RFP mice, consistent with the higher number of RFP+ cells in the BM (Figure 3A).

MFs are characterized by expression of αSMA, vimentin, and FSP1, in contrast to fibroblasts, which express collagen-α1, or stem cells, which rarely express these markers. RFP+ cells purified from the heterogeneous RFP+/− MSCs by FACS expressed all three MF markers and, thus, are distinct from RFP− cells that did not express αSMA (Figures 3F and 3G). Collagen expression was higher in the RFP− population, and αSMA expression was higher in the RFP+ population (Figure 3F); consistent with the concept that the RFP+ cells represent more differentiated MFs and that the RFP− population also differentiates into, or contains, a fibroblast-like cell type.

Analysis of the BM-derived MSCs showed that the RFP− cells contained the true MSC. Up to 80% of the unsorted MSCs (which we will refer to herein as RFP+/− cells) and up to 80% of the once-sorted RFP− cells differentiated into adipocytes and osteoblasts when grown in differentiation-specific media (Figure 3D), whereas only ~20% of RFP+ cells were able to differentiate into these cell types. RFP− cells generated more CFUs (17 CFUs), whereas RFP+ cells formed very few (five CFUs): RFP+/− cultures were even more efficient at colony formation (42 CFUs) (Figure 3C). RFP− cells were CD44+ but did not express Sca-1, and only 2.4% expressed c-kit, but upon differentiation into a mixed RFP+/− population, the cells expressed higher levels of c-kit and Sca-1; thus, these latter markers are characteristic for the RFP+ cells (Figure S3E), consistent with recent publications (Wang et al., 2009) indicating a dynamic change in cell surface-marker expression upon culture of MSCs.

We next established a lineage relationship in the production of αSMA+ cells from MSCs and demonstrated that RFP+ cells were derived from RFP− cells (schematic illustration in Figure 4D). After a first sorting and isolation of RFP− cells, cultures of RFP− cells generated new RFP+ cells and RFP− cells in the same proportion with increasing numbers of RFP+ cells over time (Figure 4A). Sorted RFP+ cells generated more RFP+ cells, but not RFP− cells (Figure 4A); after ten PDs they became senescent (Figure 4B). Interestingly, after 80 days of in vitro culture, RFP− and RFP+/− cells became tetraploid (Figure S3F) but maintained a normal karyotype in contrast to previous reports (Izadpanah et al., 2008). These data suggest that RFP− cells give rise to RFP+ cells, but not vice versa (Figure 4E; Movie S1).

RFP− cells showed superior self-renewal properties compared to RFP+ cells (Figure 4B), consistent with the RFP− cells being the progenitor to RFP+ cells. To generate pure RFP− cells, we carried out multiple (three to five) sortings of RFP− cells until we could not detect any RFP/αSMA+ cells in the population. When MSC cultures were maintained in an

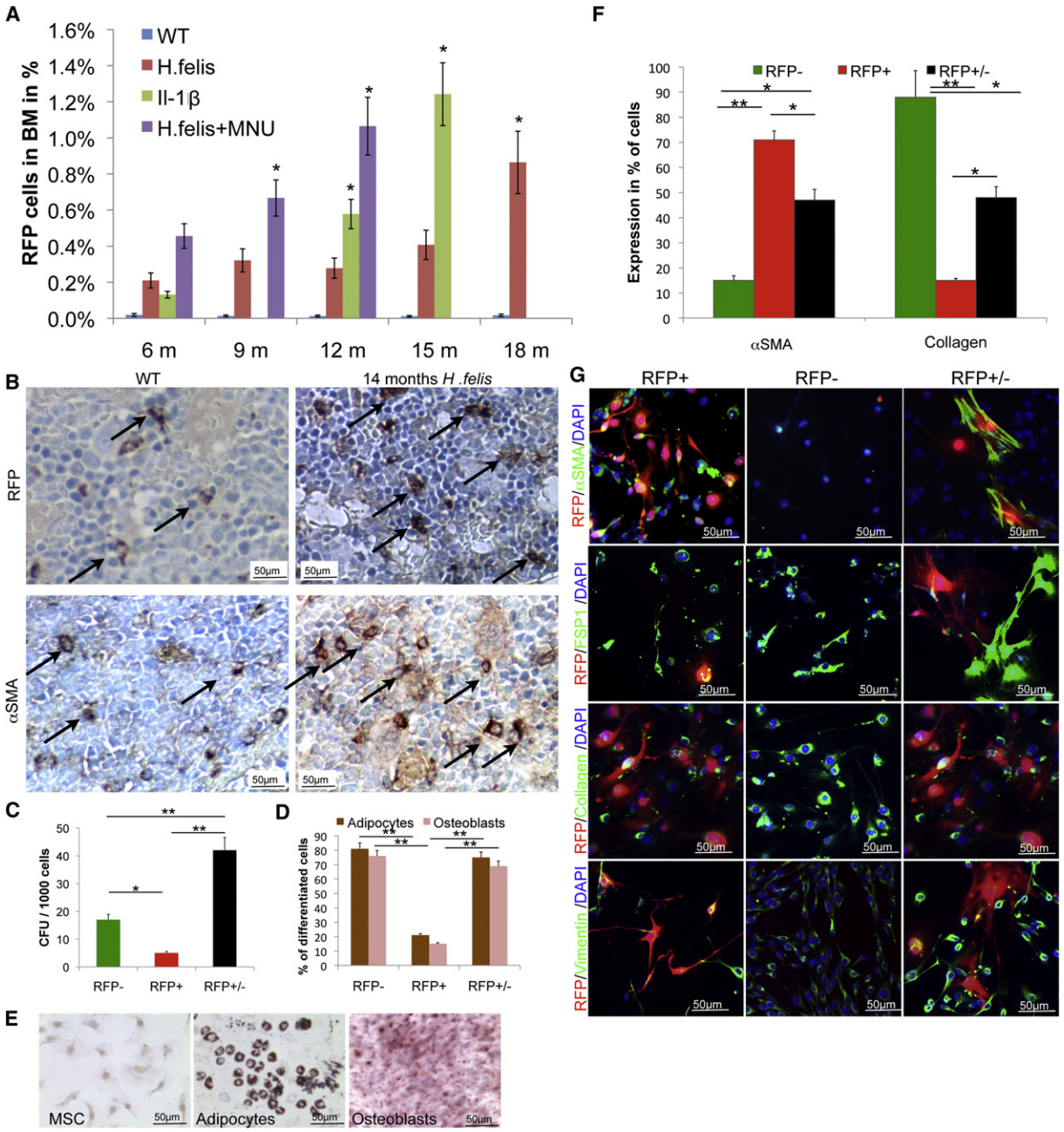

Figure 3. In a Mixed Population of MSCs, the αSMA-RFP– Cells Contain the Stem Cells, and RFP+ Cells Express a Typical MF Marker

(A) FACS for αSMA-RFP+ cells in freshly isolated whole BM of 6, 9, 12, 15, and 18-month-old αSMA-RFP+ mice with (red) or without *H. felis* infection, 6, 12, and 15-month-old IL-1β/αSMA-RFP+ transgenic mice (green), and 6, 9, and 12-month-old αSMA-RFP+ mice with *H. felis* infection and MNU treatment (purple).

(B) αSMA and RFP staining of the BM of C57/B6 (lower row) or αSMA-RFP (upper row) mice before (control) and after 14 months of *H. felis* infection. Arrows indicate cells staining positive.

(C) CFUs from 1000 plated RFP+ (red), RFP− (green), or RFP+/− (black) cells were counted after 14 days culture.

(D) Adipocyte (brown) and osteoblast (orange) differentiation of RFP+, RFP−, or RFP+/− cells was measured after 14 days culture in differentiation medium. After oil red O or alizarin red S staining, percentage (%) of differentiated cells was calculated.

(E) Representative pictures of RFP+/− cells after differentiation experiments (left as control) and after adipocyte (middle, with oil red O staining) or osteoblast (right with alizarin red S staining) differentiation.

(F) Quantitative expression of αSMA or collagen in RFP+ (red), RFP− (green), or RFP+/− (black) cells at passage 5 after a single RFP sorting. (G) Representative pictures of αSMA, FSP1, collagen, and vimentin staining in RFP+, RFP−, or RFP+/− cells. *$p < 0.05$; **$p < 0.01$.

Data are represented as mean ± SEM (see also Figure S3).

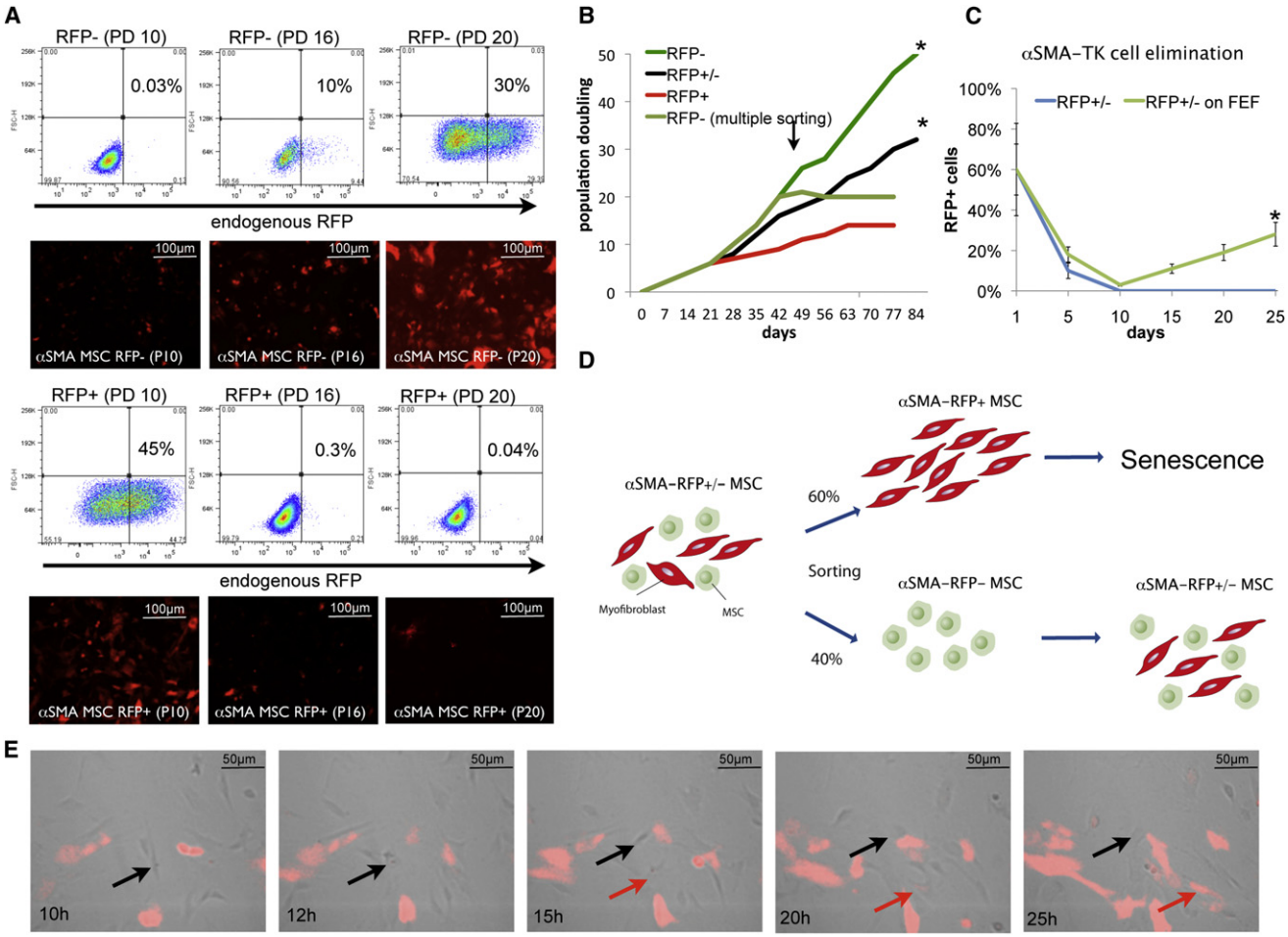

Figure 4. αSMA-RFP– Stem Cells Give Rise to Their αSMA-RFP+ Niche Cells

(A) After sorting of αSMA-RFP+ MSCs after six PDs, RFP− cells (upper panel) and RFP+ cells (lower panel) were cultured separately, and RFP expression of each population was determined. Pictures below the FACS blots represent each respective population.

(B) PDs of RFP+ (red), RFP− (green), and RFP+/− (black) cells after multiple sorting to eliminate RFP+ cells (light green). RFP expression status is shown in the red bar below the graph ("*" indicates potential tetraploidy after more than 80 days in in vitro culture).

(C) Elimination of RFP+ cells through TK ablation. Freshly isolated MSCs (adherent BM cultures) from αSMA-RFP mice were transfected with an αSMA-TK construct and treated with 50 μM GCV. Remaining RFP− cells only proliferated after the treatment and gave rise to any RFP+ cells when cultured on feeder cells (lower panel). Data are represented as mean ± SEM.

(D) Schematic illustration of the results. MSCs (RFP− cells) give rise to MSCs and MFs (RFP+ cells). After sorting, RFP+ cells become senescent after few PDs. RFP− cells can give rise to its niche cells, RFP+ MFs, and generate a heterogeneous MSC population, consisting of RFP+ and RFP− cells.

(E) Representative time-lapse microscopy images of a RFP− cell (black arrow) giving rise to RFP− (black arrow) and RFP+ (red arrow) cells in a population of RFP+/− cells. Elapsed time (from start of the microscopy, 12 hr after seeding) is indicated.

See also Movie S1, Table S2, and Figure S4.

RFP− state, the cells became senescent after a few passages, indicating that RFP+ cells are needed for RFP− cell survival. Multiple-sorted RFP− cells could be prevented from senescence by the addition of RFP+ cells (data not shown), suggesting that the senescence phenotype was not due to cell damage from sorting but, instead, due to the absence of secreted factors by RFP+ cells. To confirm these observations we transfected RFP+/− cells with a 3 kb αSMA-thymidine kinase (TK) construct (Figure S4) in order to eliminate αSMA+ cells from the population. Freshly isolated RFP+/− MSCs, transfected with αSMA-TK, and treated for 10 days with gancyclovir (50 μM GCV), showed a complete and irreversible loss of RFP+ cells, followed by loss of RFP− cells (Figure 4C). In contrast, freshly isolated and αSMA-TK transfected RFP+/− cells grown on fetal fibroblasts (FEFs) (Okawa et al., 2007) survived and generated new RFP+ cells 1–2 days after GCV treatment (Figures 4C; Figure S4B). These data indicate that RFP− stem cells can only survive in a heterogeneous population of RFP− and RFP+ cells and that the RFP+ cells probably function as niche cells for the RFP− stem cells from which they derived.

TGF-β Induces αSMA Expression in RFP– MSCs through CXCR4/SDF1α and Upregulates Gremlin-1

To investigate mechanisms by which BM- and MSC-derived MFs are induced during progression to dysplasia, we examined the effect of growth factors on RFP+ MF production.

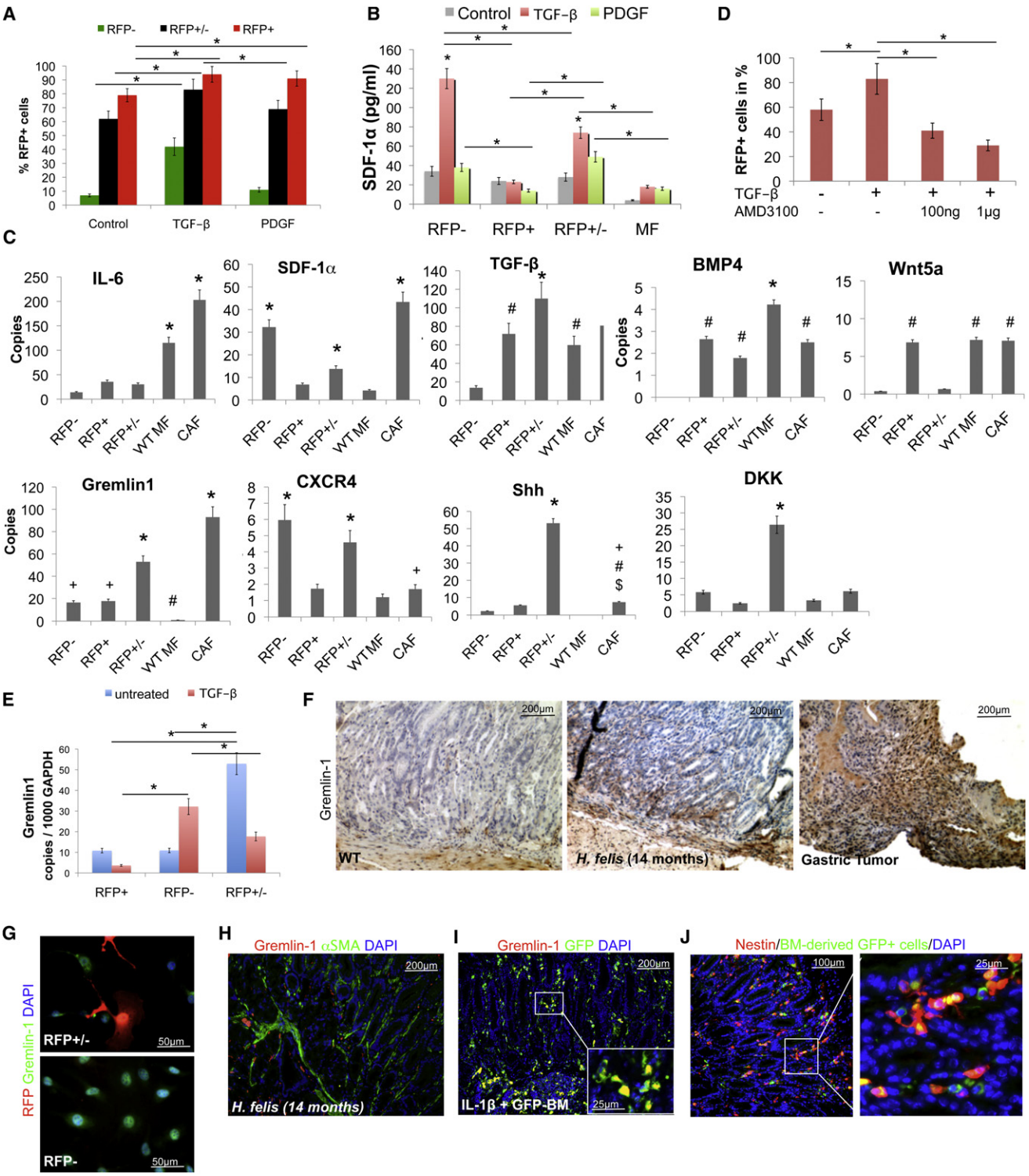

Figure 5. Regulation of the Stem Cell Niche in the BM and Tumor

(A) Percentages of RFP+ cells in populations of RFP+ (red), RFP− (green), and RFP+/− (black) cells after incubation with TGF-β or PDGF.

(B) Results of ELISA for SDF-1α expression in RFP+, RFP−, RFP+/−, and WT gastric MFs with and without incubation with TGF-β or PDGF.

(C) Gene expression data from BM MSC cultures (RFP+, RFP−, RFP+/−), CAFs, and WT MFs. qRT-PCR for expression of IL-6, SDF-1a, TGF-β, BMP4, Wnt5a, Shh, Dkk1, Gremlin 1, and CXCR4 from in vitro culture of RFP−, RFP+, RFP+/− cells, gastric RFP+ CAFs, and WT gastric MFs as a control (copies are calculated per 10,000 copies of GAPDH; *$p < 0.05$ compared to all other cells, #$p < 0.05$ compared to RFP− cells, \$$p < 0.05$ compared to RFP+ cells, +$p < 0.05$ compared to MFs [Dunnett test for multiple comparisons]).

We stimulated unsorted or sorted MSC cultures with TGF-β or PDGF, which have been strongly linked to MF differentiation. In all cell populations (RFP+, RFP−, and RFP+/− cells), RFP/αSMA expression was strongly stimulated by TGF-β and to a lesser extent by PDGF, with the greatest effect on the RFP− population (Figure 5A; Figure S5A). In addition, growth factor stimulation resulted in more rapid proliferation of RFP+ cells (Figures S5A and S5B).

Next, we examined factors expressed by RFP+ cells that might contribute to the BM niche and tumor microenvironment. IL-6 has been associated with the development of gastrointestinal cancer (Grivennikov et al., 2009). BM-CAFs and WT MFs expressed high levels of IL-6 compared to parental MSCs (Figure 5C, a finding confirmed by ELISA (data not shown)). RFP+ cells also expressed higher levels of BMP4 and Wnt5A (factors known to contribute to the stem cell niche) and exhibited a CAF-like gene expression pattern (Figure 5C). This inflammatory gene expression profile correlated with analyses of BM-derived GFP+ gastric CAFs compared to the total gastric CAF population (Table S1). SDF-1α, which has been associated with stromal-dependent cancer progression, was highly expressed in RFP− cells compared to WT MF or RFP+ cells (Figures 5B and 5C). Thus, it seems likely that SDF-1α is expressed by MSCs rather than CAFs and may represent a mechanism by which MSCs regulate MF proliferation or recruitment to the niche.

Therefore, we examined the effect of TGF-β stimulation on SDF-1α production by MSC. Incubation with TGF-β increased SDF1α production 5-fold in RFP− cells (Figure 5B), but not in RFP+ cells or WT MFs. TGF-β-mediated induction of proliferation and differentiation in MSCs was inhibited by the CXCR4 antagonist AD3100 (data not shown) because CXCR4 was mainly expressed on RFP− and RFP+/− cells (Figure 5C). AMD3100 reduced TGF-β-induced differentiation of RFP+/− cells into RFP+ cells in a dose-dependent matter (Figure 5D; Figure S5C). Thus, TGF-β can induce MF differentiation of MSCs in part through upregulation of SDF1α in MSCs. Migration of cancer cells induced by BM-derived gastric IL-1β-MFs was significantly increased compared to WT MFs, and this effect could be inhibited by blocking CXCR4 (Figure S5D).

The BMP antagonist Gremlin-1 was upregulated during gastric carcinogenesis (Figure 5F) but was expressed at low levels in RFP− and RFP+ cells (Figure 5E). Interestingly, though, Gremlin-1 was upregulated in RFP+/− cells, suggesting that Gremlin-1 is induced by an interaction between RFP+ and RFP− cells. Gremlin-1 was highly expressed in CAFs, but not in WT MFs (Figures 5C and 5E), and TGF-β upregulated Gremlin-1 expression in RFP− cells, but not in RFP+ cells (Figure 5E). In RFP+/− cells, Gremlin1 could only be detected in RFP− cells (Figure 5G), and αSMA and Gremlin-1 did not overlap in CAFs in gastric dysplasia (Figure 5H), indicating that Gremlin-1 is likely a marker of MSCs in their niche in the BM and tumor microenvironment. IHC revealed that the majority of Gremlin-1+ cells in IL-1β-mice transplanted with EGFP-BM were GFP+ (Figure 5I), indicating that Gremlin-1+ cells were largely BM derived. A recent study (Mendez-Ferrer et al., 2010) reported Nestin1 as a marker for MSCs in the BM, where MSCs contribute to the BM niche for HSCs. We observed colocalization of a subpopulation of Nestin1+ and GFP+ BM-transplanted stromal cells in gastric dysplasia (Figure 5J), confirming that BM-derived MSCs are present in the dysplastic stomach. Sonic hedgehog (Shh), which regulates stem cells, and Dickkopf-1 (DKK1), an inhibitor of the Wnt pathway, were also expressed mainly in RFP+/− cells, reflecting an active niche environment (Figure 5C).

BM-Derived MFs from Gastric Dysplasia or MSCs Induce Invasive Growth of Gastric Tumor Cells in a 3D Organotypic Model

Given the evidence that CAFs originate from BM-MSCs and are recruited to the stomach at early stages of dysplasia, we investigated interactions between tumor cells and CAFs. When cocultured with the human gastric cancer cells, AGS, RFP−, RFP+, and RFP+/− cells all increased the expression of RFP/αSMA (Figure 6A), along with the MF markers FSP1 and vimentin (data not shown). In contrast, expression of collagen was downregulated in RFP− and RFP+/− cells to approximately the level found in RFP+ MFs (Figure 6A). Thus, coculture with tumor cells induces differentiation of MSCs toward the myofibroblastic lineage. In coculture experiments, SDF-1α levels were significantly decreased in all stromal cell populations (Figure 6B), particularly in the RFP− cells, consistent with increased differentiation of MSCs into αSMA+ MFs.

To study the biologic effects of BM- and MSC-derived MFs on tumor cells, we used a 3D organotypic cell culture system: AGS cells were laid onto an extracellular matrix (ECM) gel mixture with MSC-derived cell populations (RFP−, RFP+, and RFP+/− cells), normal WT gastric MFs, gastric CAFs, or BM-CAFs (Figures 6C and 6D). When placed on WT MFs, AGS cells grew with minimal signs of invasion, as expected for a well-differentiated, weak tumorigenic cell line in organotypic culture (Figure 6D). In contrast, when cultured on pooled gastric CAFs, tumor cell invasion into ECM could be detected (Figure 6D). However, AGS cells cultured on the RFP+ cells (19 invasion sides/cm), the RFP+/− cells (eight invasion sides/cm), and the IL-1β BM-derived CAFs (seven invasion sides/cm) revealed high levels of invasion into ECM (Figures 6C and 6D). In contrast, nearly no invasion was observed when AGS cells were cultured on RFP− cells.

Given recent findings that widespread hypomethylation characterizes CAFs from human gastric tumors and from a transgenic

(D) Quantitative analysis of the dose-dependent effect on RFP expression in RFP+/− after 48-hr incubation with TGF-β and 100 ng/ml (left) or 1 μg/ml (right) of the CXCR4 inhibitor AMD3100.
(E) qRT-PCR for Gremlin-1 expression in RFP+, RFP−, and RFP+/− cells with (red) and without (blue) 48-hr incubation with TGF-β.
(F) Representative picture of Gremlin-1 staining of WT mouse stomach (left) and mouse stomach with gastric dysplasia after 14 months of *H. felis* infection (middle), and invasive gastric cancer in 14-month-old IL-1β mice (right).
(G) Representative pictures of Gremlin-1 staining (green) of RFP+/− and RFP− cells (left, RFP [red] is endogenous αSMA-RFP).
(H) Representative double staining for Gremlin-1 (red) and αSMA (green) in gastric dysplasia in 18-month-old *H. felis*-infected mice.
(I and J) Representative picture of Gremlin1 (I) and Nestin1 (J) staining in 12-month-old GFP-BM transplanted IL-1β mice. *$p < 0.05$.
All data are represented as mean ± SEM (see also Figure S5).

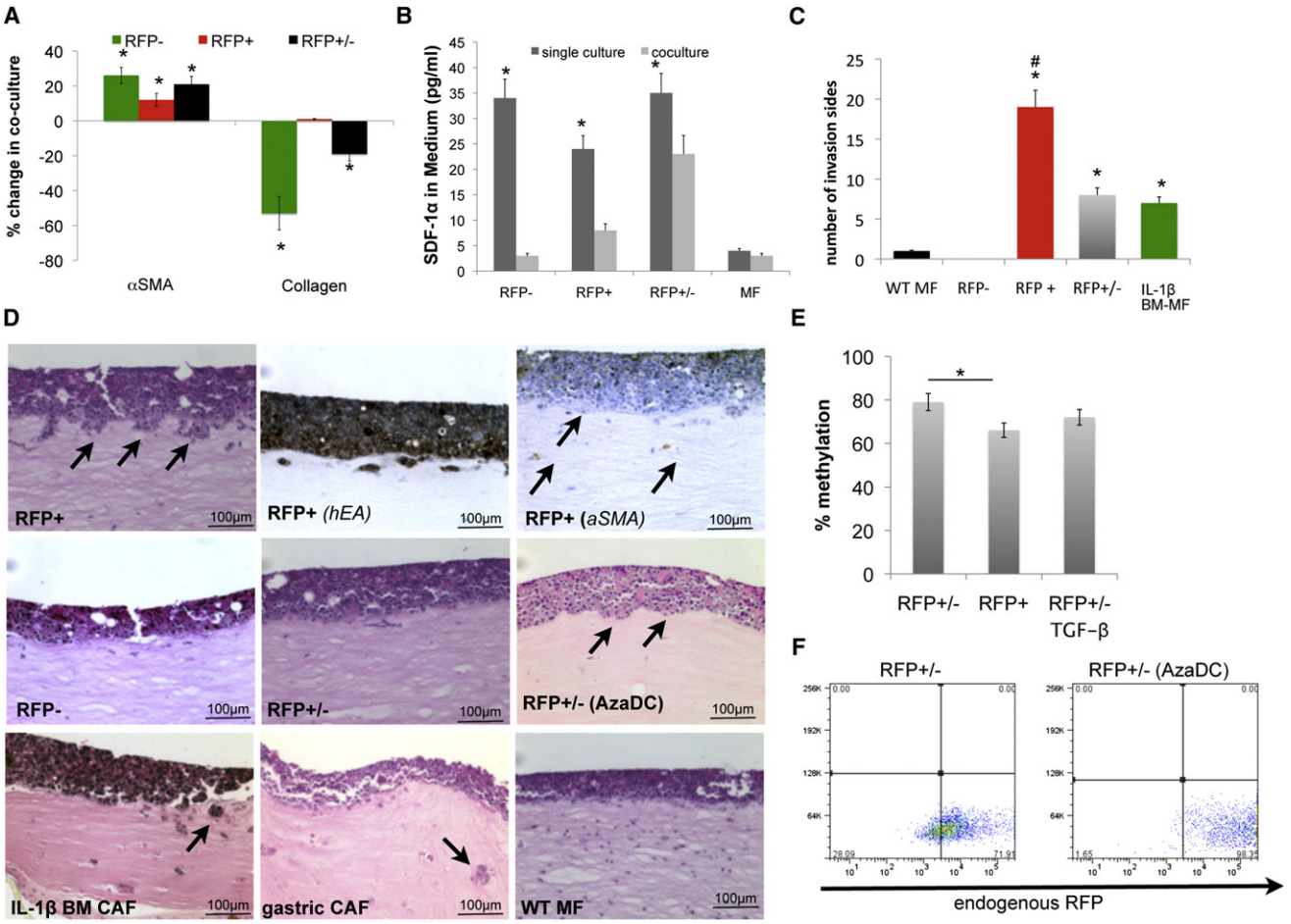

Figure 6. MF Differentiation of MSCs Promotes In Vitro Tumor Invasion

(A) Percent (%) change of αSMA and collagen expression in RFP−, RFP+, and RFP+/− cells cocultured with AGS or MKN45 gastric tumor cells (see Figure 3D for controls; *$p < 0.05$).

(B) Results of ELISA for SDF-1α expression in RFP+, RFP−, and RFP+/− cells in single or coculture with AGS gastric tumor cells.

(C) Quantification of invasions per 1 cm from organotypic culture experiments in RFP−, RFP+, and RFP+/− cells of WT MFs and IL-1β-BM MFs grown in a 3D collagen/Matrigel matrix with AGS on top (*$p < 0.05$ compared to WT MFs and #$p < 0.05$ compared to RFP+/− or IL-1β MFs).

(D) Representative pictures of organotypic culture with AGS cells growing on top of a 3D collagen/Matrigel matrix that contains different cell populations. Upper panel shows RFP+ cells (arrows indicate invasion sites) with representative pictures of the staining for human epithelial antigen (hEA) to detect human AGS cells (middle) or αSMA to detect the αSMA-RFP expressing cells in the matrix (arrows at right). Middle panel indicates AGS cells on RFP− (left) or RFP+/− (middle) cells, and on RFP+/− cells after incubation with 5-azacytidine (35 μl/ml) for 10 days. Lower-left panel shows IL-1β BM MFs; lower-middle panel illustrates isolated gastric CAFs from mice after 18 months of *H. felis* infection; and lower-right panel indicates WT, uninfected gastric MFs.

(E) Relative methylation in the cytosine extension assay of RFP+/− and RFP+ cells compared to RFP+/− cells treated with TGF-β for 48 hr.

(F) FACS for RFP expression in RFP+/− cells before (left) and after (right) incubation with 5-azacytidine for 10 days and six PDs. *$p < 0.05$.

All data are represented as mean ± SEM.

mouse model of multistage gastric carcinogenesis (Jiang et al., 2008), we examined the role of methylation in development of RFP+ cells. We observed significantly ($p < 0.05$) higher levels of DNA methylation in RFP+/− than in RFP+ cells (Figure 6E), supporting the concept that development of RFP+ MFs is regulated in part by hypomethylation. Incubation of mixed RFP+/− MSCs with 5-aza-dC induced DNA demethylation, increased the proportion of RFP+ cells (Figure 6F), and increased the degree of tumor cell invasion in the organotypic model (Figure 6D). Interestingly, TGF-β also induced hypomethylation in RFP+/− cells (Figure 6E). These findings indicate that hypomethylation of RFP+/− cells from the BM can contribute to the development of a CAF phenotype, might be sufficient to further transform non-tumorigenic tumor cells, and contributes to tumor invasion.

BM- and MSC-Derived MFs Induce Tumor Growth In Vivo When Injected Locally or at a Distance

To confirm the findings from the organotypic model, we analyzed the effects of BM- and MSC-derived MFs in xenograft tumor models. When 10^5 MKN45 cells were injected, there was only minor tumor growth after 6 weeks, but tumors were observed with 10^6 MKN45 cells, or when 10^5 MKN45 cells were coinjected with stromal cells (Figures S6A and S6B). Coinjection of 10^5 MKN45 cells with FEFs, or RFP− MSCs, resulted in small

tumors. Large tumors were observed when 10^5 MKN45 cells were coinjected with RFP+, RFP+/−, or IL-1β-BM-CAFs (Figures S7B and S7D). The nontumorigenic AGS cells formed tumors only in combination with RFP+ or IL-1β-BM-CAFs using the same number of cells (10^5 or 10^6, Figure S6C). Preliminary experiments with mouse pancreatic cancer cells and CAFs confirmed those findings (data not shown). These in vivo data support the conclusions from organotypic assays that BM- and MSC-derived RFP+ cells contribute to tumor growth and have properties that are distinct from normal fibroblasts and MFs.

To further examine the in vivo importance of MSCs to the CAF population, we injected MKN45 cells into both flanks of a mouse but injected only one flank with IL-1β-BM-CAFs (GFP+), WT MFs, gastric CAFs (HF-MF), or RFP+, RFP−, or RFP+/− cells. Flanks injected with cancer cells along with RFP− cells or WT MFs developed small tumors, whereas the opposite flanks injected with only cancer cells did not develop tumors (Figure S6D). Coinjection of cancer and RFP+ cells resulted in formation of large tumors on the flank of coinjections and small tumors on the other flank. Interestingly, coinjection of cancer cells and RFP+/− cells, gastric CAFs (HF-MF), or IL-1β-BM-MF cells resulted in formation of large tumors on both flanks (Figures 7A and 7B). These findings indicate that CAFs that contain MSCs and myofibroblastic cells are likely able to promote tumor growth at distant sites. When we injected one flank with 10^5 MKN cells and IL-1β-BM-CAFs (without tumor cells) on the opposite flank, we observed increased tumor growth as with injections on the same flank (Figures 7B and 7C). Similar results were observed with IL-1β-BM-MFs injected intraperitoneally (Figure S6E). IHC for αSMA showed an increased number of MFs in the large tumors with coinjections of RFP+ or RFP+/− cells, compared to those of RFP− cells, FEFs, or WT MFs (Figures 7A and 7B). RFP or GFP expression was detected in large tumors on both flanks by IHC (Figure 7A, white arrows) and PCR (Figure S6F); RFP and GFP primarily colocalized with αSMA expression in mice that received coinjections of tumor and RFP+ and RFP+/− cells, or IL-1β-BM-CAFs. Interestingly, not all GFP-labeled IL-1β-BM-MFs expressed αSMA (Figures 7A and 7B, orange arrows), consistent with the notion that these CAF preparations were similar to the RFP+/− population, containing MFs and MSCs.

To determine if endogenous BMDCs also contributed to the observed tumor growth, we performed experiments with WT C57/B6 mice transplanted with BM from αSMA-RFP mice or UBC-GFP mice (Figure S6H). Chimeric mice with the UBC-GFP BM were given injections of RFP+/− cells together with syngeneic 10^5 TC-1 murine cancer cells in one flank and TC-1 cells alone on the other. Mice with αSMA-RFP BM received coinjections of GFP+ IL-1β-BM-MFs and TC-1 cells in one flank and only TC-1 cells in the other (Figure S6H). Again, we observed increased tumor growth with coinjections (data not shown), compared to only tumor cells; and stromal cells were recruited to the tumors. Tumors contained multiple BM-derived GFP+ or RFP+ cells, including αSMA+ MF-shaped cells (Figure S6H). Interestingly, coinjection of MSC-containing CAF preparations significantly increased the number of GFP+ BMDCs and RFP+ MFs in tumors, in contrast to few GFP+ cells in tumors of mice not given coinjections (Figures S6G and S6H). Thus, the recruitment of BM-derived CAFs can be accelerated by the presence of MSCs in the tumor microenvironment. Taken together, BM- and MSC-derived αSMA+ MFs can be recruited to the tumor to stimulate growth, but the combination of the RFP+ myofibroblastic cells and RFP− MSCs, which recreate the BM niche at the tumor site, is a particularly potent stimulant of tumor growth and responsible for further recruitment of BMDCs (see model: Figure 8G).

CXCR4/SDF1 Contributes to Migration of BM-Derived MFs to the Tumor, Whereas TGF-β Inhibition Decreases MF Differentiation In Vivo

Having shown that SDF-1α signaling modulated MF differentiation in vitro, we analyzed the importance of SDF-1α signaling in vivo. We coinjected GFP-labeled IL-1β-BM-MFs with MKN45 cells in one flank, and MKN45 cells alone in the other flank, and then administered a TGF-β receptor 2 (R2) inhibitor (SB-505124) or CXCR4 inhibitor (AMD3100) for 6 weeks. Mice given the TGF-βR2 inhibitor developed smaller tumors on both flanks (Figures 8A and 8B), compared with untreated control mice (Figure 8A). IHC revealed a decrease in total GFP-labeled and αSMA+/GFP+ MFs, suggesting less differentiation of MSCs to CAFs, consistent with the in vitro results. In mice that were given the CXCR4 inhibitor, we observed a slight decrease in tumor size on the flank that received coinjection of IL-1β BM-MFs and MKN45 cells but very small tumors on the flank only injected with tumor cells (Figures 8A and 8B). IHC revealed no GFP+ cells with few if any αSMA-expressing MFs on the contralateral side, and a reduced number of non-GFP αSMA+ cells on the coinjection side (Figure 8A). These findings indicate that SDF-1α signaling is likely required for the recruitment and migration of MSCs or MFs to the tumor site.

To extend these findings, we treated *H. felis*-infected αSMA-RFP mice (12 months) with the CXCR4 inhibitor (5 mg/kg/day AMD3100 in four consecutive Alzet© mini pumps) for 4 months and analyzed the effects on gastric carcinogenesis and αSMA/RFP+ BMDCs. CXCR4 antagonism resulted in a marked reduction in αSMA+ cells in the BM of the treated mice, which seemed to be replaced by fat cells (Figures 8E and 8F); it led to a reduction in gastric αSMA+ cells (Figure 8C) and inhibited the development of gastric dysplasia compared to untreated control mice (Figure 8D). The findings are consistent with the model in which targeted inhibition of BM αSMA+ MF production reduces cancer progression, although we cannot completely exclude a direct effect of the CXCR4 antagonist on the development of dysplasia.

DISCUSSION

Although it is widely accepted that tumorigenesis is regulated by interactions between tumor cells and CAFs, the precise origin and function of CAFs have been unclear. We show that: (1) CAFs increase during chronic inflammation and gastric cancer progression, particularly during the transition to dysplasia; (2) CAFs are derived from αSMA+ MFs present in the normal BM; and (3) αSMA+ MFs are generated from MSCs and contribute to the normal BM niche and MSC self-renewal. During chronic inflammation and carcinogenesis, these αSMA+ BM niche cells are expanded in a TGF-β-dependent matter and recruited through CXCR4/SDF1α signaling together with Gremlin-1-expressing MSCs to incipient tumors where they contribute to a tumor niche that promotes and sustains tumor progression.

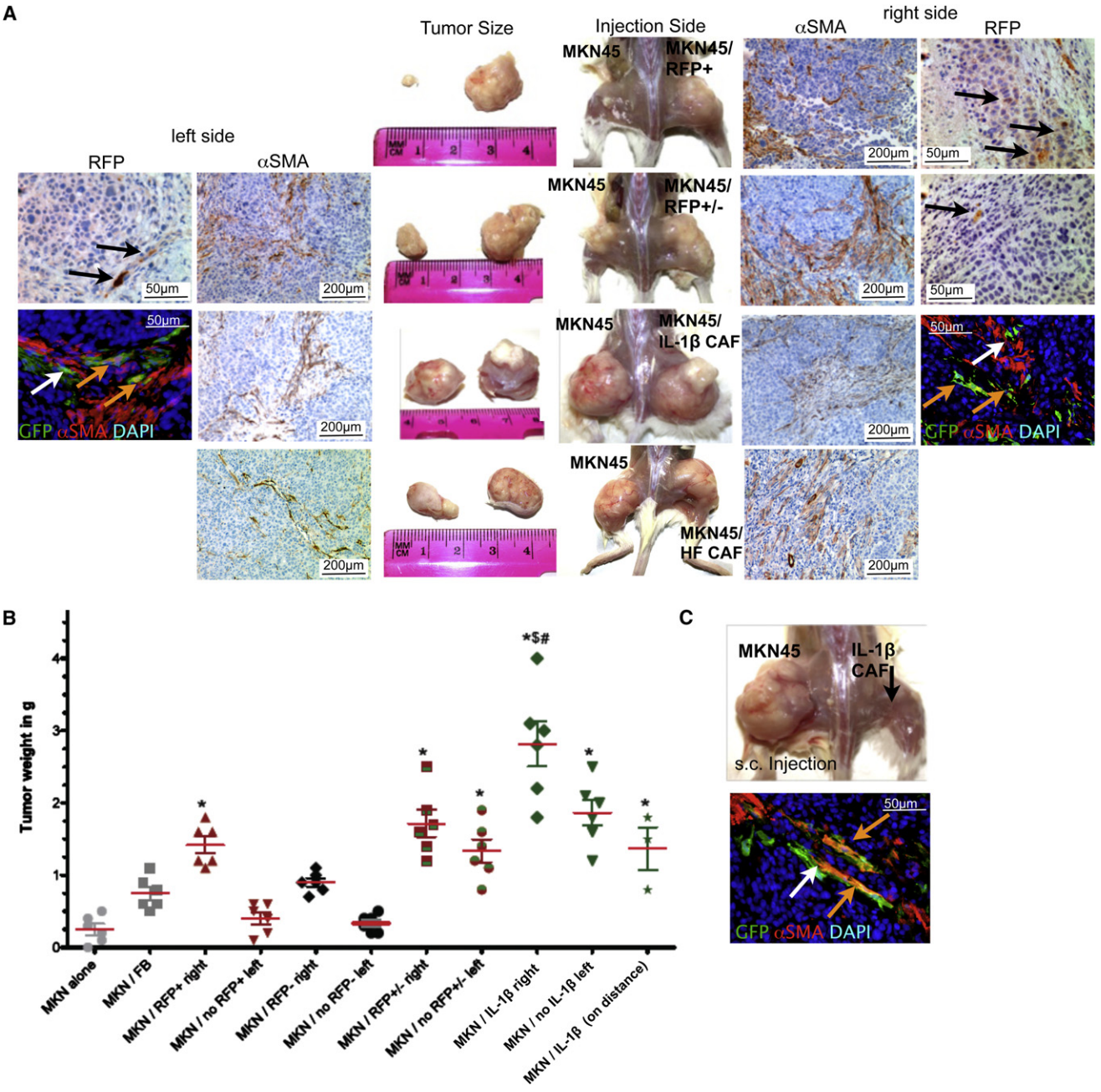

Figure 7. BM-Derived Gastric MFs and Heterogeneous MSCs Promote Xenograft Tumor Growth

(A) For xenograft experiments (from top to bottom), 10^5 RFP+, RFP+/−, IL-1β-BM MF, and gastric RFP+ CAFs were coinjected with 10^5 MKN45 cells on the right flank, and 10^5 MKN45 cells were injected alone on the left flank of SCID mice. Tumor injection sites and tumor sizes and representative images of staining for αSMA and RFP or GFP are shown. IHC, orange arrows indicate double staining, and white arrows indicate only GFP expression.

(B) Quantification and statistical analysis of xenograft experiment of 10^5 fibroblasts (FB), RFP+, RFP−, RFP+/−, and IL-1β-BM MFs after coinjected with 10^5 MKN45 on the one side, but only tumor cells on the contralateral side. IL-1β-BM MFs were injected at a distant site, and 10^6 MKN cells were injected into the contralateral flank. (*$p < 0.05$ compared to MKN alone, #$p < 0.05$ compared to RFP+ and RFP+/− cells, and $$p < 0.05$ compared to RFP− and FB [Dunnett; all data are represented as mean and measure points].)

(C) RFP+/− cells or IL-1β-BM-CAFs were injected s.c. in a mouse with a tumor of 10^6 MKN cells growing on the left flank. IHC for αSMA (green) and endogenous RFP show double staining (orange arrows) or only αSMA expression (white arrow) in the tumor.

See also Figure S6.

In inflammation-dependent models of gastric cancer, progression to dysplasia is associated with accumulation of αSMA-expressing CAFs, compared to collagen-α1-expressing fibroblasts. αSMA-expressing CAFs could in theory originate from local fibroblasts, endothelial cells, mesenchymal cells, local epithelial cells during the EMT, or recruited BMDCs. Studies

using RIPTag transgenic mice showed that BMDCs can give rise to CAFs and fibroblasts (Direkze et al., 2004), which was confirmed in other cancer models (Guo et al., 2008). More importantly, studies in patients with gastric cancer that received gender-mismatched BMTs have confirmed the BM origin of CAFs in gastric cancer (Worthley et al., 2009). We demonstrate through BM reconstitution studies in mice that 20% of αSMA+ fibroblastic cells that accumulate in dysplasia are BM derived and that BM MSCs are the likely origin of these CAFs (Figure 8G). In contrast to previous reports (Simmons et al., 1987; Yokota et al., 2006), we show here that it is indeed possible to transplant BM MSCs in the mouse. CAFs recruited from the BM are functionally more active as promoters of tumor growth and invasion compared to normal or resident fibroblasts, and exhibit a previously reported NF-κB-dependent inflammatory gene expression signature (Erez et al., 2010), which accounts for higher levels of pro-inflammatory cytokines in CAFs (Karnoub et al., 2007; Orimo et al., 2005).

In mouse models of inflammation-induced gastric dysplasia, αSMA+ CAFs were recruited to the stomach after first accumulating in the peripheral blood and in the BM. Indeed, the accumulation of αSMA+ cells in the BM appeared to correlate with the development of dysplasia, and suggests that carcinogenesis involves an early stage of BM remodeling. In the normal BM, MSCs are able to give rise to αSMA+ cells that morphologically and functionally behave identically to CAFs isolated from the dysplastic stomach, and these αSMA+ MF cells appear to be expanded in cancer.

Previous studies have suggested that MSCs can be induced to differentiate into CAFs, particularly when exposed to tumor-conditioned media (Mishra et al., 2008). However, we show that differentiation of MSCs into αSMA+ cells is a normal pattern of differentiation in vitro and in vivo, compatible with asymmetric stem cell division in a broad definition, although more specification regarding an intrinsic or extrinsic mechanism would be needed (Morrison and Kimble, 2006). Moreover, αSMA+ myofibroblastic cells represent normal niche cells within the BM that maintain the self-renewal properties of MSCs. In culture, MSCs lose their proliferative potential and ability to self-renew when αSMA+ cells are specifically eliminated, and these capabilities are restored if αSMA+ cells are added back to the MSC. The αSMA-RFP transgene has allowed us to sort the heterogeneous, adherent population of BM mesenchymal cells, revealing that the true MSC is αSMA−but can give rise to αSMA+ MFs.

Most adult stem cells are extremely difficult to culture in vitro in the absence of supportive niche cells or defined growth factors, and the fact that MSCs generate their own αSMA+ niche cells clarifies the self-renewal abilities of BM MSC cultures. The concept that a stem cell is able to generate its own niche cell has precedence (Mathur et al., 2010; Snippert et al., 2010). In addition the presence of the αSMA+ cells in the BM raises interesting questions regarding the possible role of these cells beyond support of the MSCs. The BM niche is thought to consist of osteoblasts (Lo Celso et al., 2009), which only exist in the bone, but further studies are required to determine if CAF-like cells support the growth of stem cells beyond the MSCs.

The development of dysplasia and tumors in the stomachs of mice was associated temporally with an expansion of αSMA+ cells in the BM, which was reproduced by coculture of MSCs with gastric cancer cells, indicating the effect of a soluble, secreted factor. Previous studies have shown that coculture of MSCs with cancer cells could result in differentiation into CAFs (Mishra et al., 2008) and that DNA hypomethylation induced by 5-aza-dC promoted the differentiation of pooled human MSC cultures into CAFs. We had shown that CAFs become markedly hypomethylated during early stages of human gastric carcinogenesis (Jiang et al., 2008). Here, we confirm that hypomethylation is sufficient to induce differentiation of CAFs and that the effect is specific for the RFP− MSCs. However, we also demonstrate that a soluble growth factor often secreted by tumors, TGF-β, may contribute to the development of CAFs from MSCs during tumorigenesis. Incubation of RFP− BM-derived MSCs with TGF-β induced DNA hypomethylation and accelerated their differentiation into αSMA+ CAFs. The promotion by TGF-β of myofibroblastic differentiation occurs in part through an SDF-1α-dependent pathway because inhibition of CXCR4 blocked this differentiation process. Thus, although global hypomethylation is a well-known feature of malignant tumors, we demonstrate that TGF-β can induce both fibroblastic differentiation and global DNA hypomethylation rapidly in vitro.

The αSMA+ MF niche cells express a number of factors that likely contribute to the stem cell niche and also maintain the self-renewal properties of incipient tumors (Figure 8G). Factors such as Wnt5a, BMP4, and IL-6 were highly expressed by RFP+ cells, as well as BM-derived CAFs isolated from gastric dysplasia. Wnt signaling has been shown in the gut to be important both for the maintenance of tissue stem cells and the generation of cancer stem cells (CSCs) (Brabletz et al., 2009) and recently was associated with maintaining or inducing stemness in CSCs (Vermeulen et al., 2010). BMPs have also been linked to intestinal and hematopoietic stem cell maintenance, controlling the stem cell number through regulation of the niche size (Zhang and Li, 2005). IL-6 appears to be required for the survival of intestinal epithelial cells and the development of inflammation-associated cancer of the gut, probably through activation of STAT-3 pathways in intestinal progenitors (Grivennikov et al., 2009). However, although the RFP+ CAFs promoted in vitro proliferation of cancer cells in organotypic models, the RFP+/− cells, which contained MSCs and CAFs, appeared to be very important in promoting in vivo tumor growth, particularly when injected at a distance from the tumor site. These findings indicate that MSCs are required for the production or migration of CAFs over time. Our results suggest that SDF-1α is likely produced by the MSC-containing RFP− population, rather than the RFP+ CAFs; SDF-1α seems to function in an autocrine function to stimulate more niche cells, and a paracrine function to attract and maintain CAFs in close proximity to tumors. Thus, CXCR4 antagonism—in our xenograft studies and our gastric carcinogenesis studies—appeared to inhibit stromal cell recruitment to the tumors and also block the production of CAFs in the BM of mice with cancer.

The two cell types (RFP− MSCs and RFP+ MFs) function together as stem cell and niche cell and communicate with each other. A crosstalk between the MSCs and MFs results in a unique pattern of gene expression characteristic of the niche, compared to those of each individual cell population. For example, DKK1 and Shh are significantly upregulated in heterogeneous RFP+/− cultures, but not in sorted RFP− and

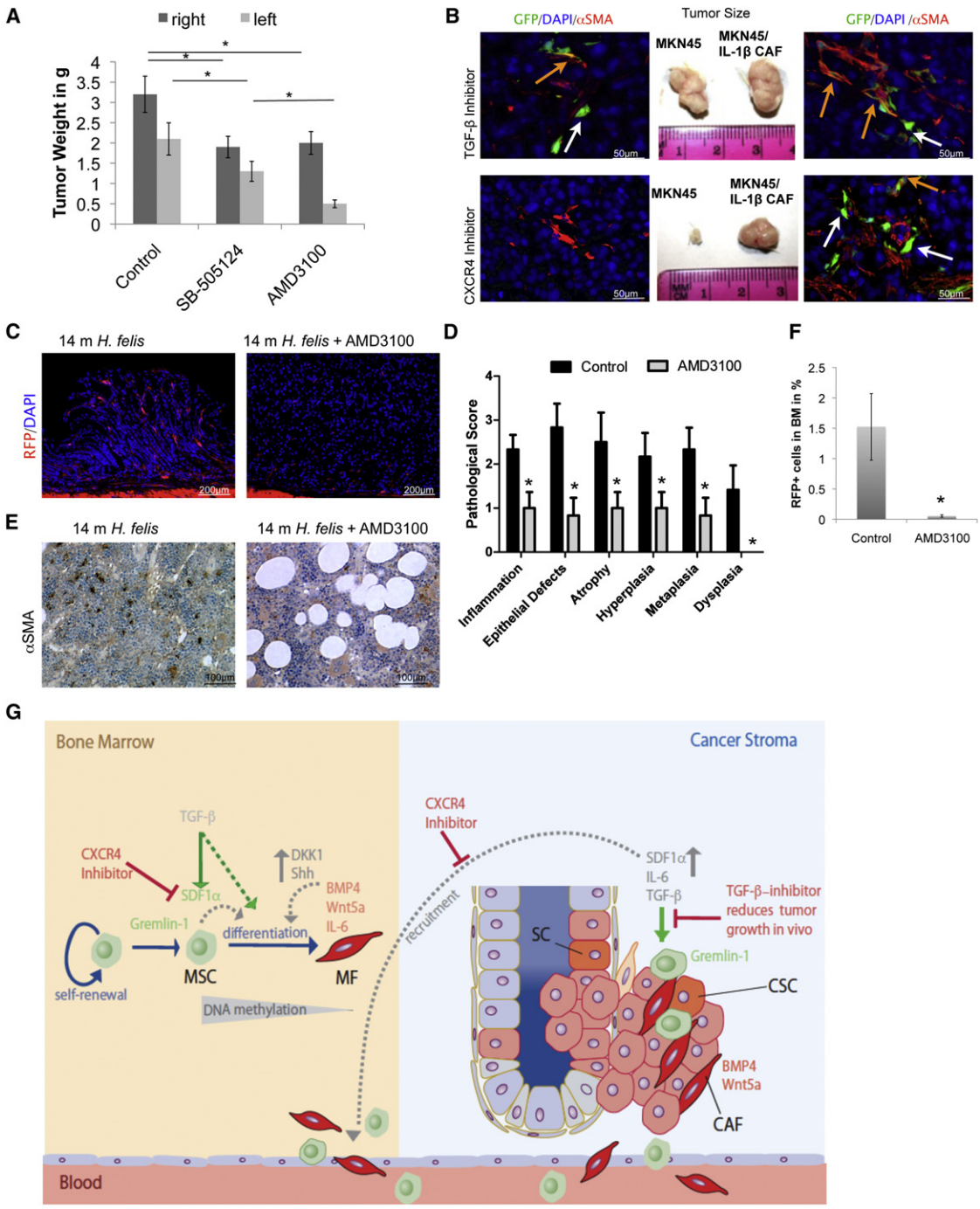

Figure 8. CXCR4/SDF1 Inhibition Reduced MF and MSC Recruitment and Tumor Growth

(A) Effects of TGF-β or CXCR4 inhibition. Quantification and statistical analysis of xenograft experiment with mice coinjected with IL-1β BM-MF and MKN45 cells on one flank and MKN45 alone on the other flank. Tumor size in grams after 6 weeks of tumor growth in mice given the TGF-βR2 inhibitor (SB-505124) or CXCR4 inhibitor (AMD3100) (*p< 0.05; Dunnett).

(B) Tumor size (middle) after 6 weeks of tumor growth in mice given the TGF-βR2 inhibitor (upper panel) or CXCR4 inhibitor (lower panel). Representative IHC of each tumor (right, left) with staining for endogenous GFP and αSMA (orange arrows indicate double staining, and white arrows indicate expression of only GFP).

(C–F) Effect of CXCR4 inhibitor treatment on stomachs of 16-month-old *H. felis*-infected αSMA/RFP mice after 4 months of AMD3100 treatment.

(C) Representative IHC of (left) untreated control and (right) AMD3100-treated mice and (D) histopathological scoring of the same experiment (*p < 0.05; n = 3).

(E) Representative pictures of (left) untreated control BM and (right) BM of AMD3100-treated mice with αSMA staining and (F) quantification of RFP+ cells in the BM by FACS (*p < 0.05; n = 3). All data are represented as mean ± SEM.

(G) Schematic drawing that depicts interactions between the BM niche (left) and the gastric cancer stroma (right). A significant portion of CAFs (red) originates from the BM and is derived from MSCs (green). The normal BM niche consists of self-renewing MSCs that give rise to MFs that resemble CAFs and likely

RFP+ cells, indicating that these factors can only be expressed in a functioning stem cell niche. Gremlin-1 was expressed on RFP− cells, presumably the true MSCs, but mainly under the conditions when the MSCs were cultured together in a mixed RFP+/RFP− population. Interestingly, Gremlin-1, an antagonist of the BMP pathway, is not expressed by normal adult fibroblasts or MF from the skin or most solid organs; expression of Gremlin-1 has been reported to be unique to stromal cells in the setting of cancer (Sneddon et al., 2006) and was consistently upregulated in our model of gastric carcinogenesis. Because Gremlin-1 expression was observed only in cultures that contain MSCs and MFs/CAFs, it is possible that MSC expression of Gremlin-1 occurs in response to BMP signals from the αSMA+ myofibroblastic cells. Consistently, high levels of Gremlin-1 have been observed in mouse embryonic fibroblast cells that are capable of maintaining human embryonic stem cells in culture (Pera et al., 2004).

In summary, we show that chronic inflammation and epithelial dysplasia lead to remodeling of the BM and expansion of αSMA+ MFs in a manner that promotes cancer growth and progression. The CAF-like MFs contribute to the niche for the MSCs, and it is this fully intact MSC niche that is recruited to the tumor site and that stimulates malignant progression. The recruitment of the niche to the tumor site can be blocked by CXCR4 inhibition, and the differentiation of MSCs can be abrogated by TGF-β inhibition. We propose a model in which during the earliest stages of inflammation-induced tumor development, the BM undergoes remodeling, mediated in part by TGF-β, and then the MSC-CAF stem cell niche promotes tumor progression through SDF-1α signaling (Figure 8G). These observations have implications for the early diagnosis and treatment of cancer.

EXPERIMENTAL PROCEDURES

Isolation and Culture of Cells

BM cells were collected by flushing femurs of αSMA-RFP mice. MSCs were cultured in murine mesenchymal medium with supplements (MesenCult). Serial cultures of the different MSCs were performed in 10 cm dishes by plating 10^5 cells, refeeding the cells every other day, and subculturing every 4–5 days. The doubling number of each passage was calculated with the formula $PD = (n_f/n_0)/\log 2$. WT (WT MFs), BM-derived (BM-MFs), and αSMA-RFP MFs (RFP-MFs) were isolated from the stomach of C57BL/6, IL-1β/αSMA-RFP, and αSMA-RFP reporter mice. Stomachs were cut into small pieces that were incubated with collagenase I at 37°C for 1 hr. Cells were filtered with a cell strainer and washed with PBS. Harvested cells were cultured in RPMI medium without Glutamine, supplemented with 10% FBS (Hyclone) and penicillin-streptomycin at 37°C in 5% CO_2. Characteristic features of MFs (abundant myofibrils with dense bodies, indented nucleus, basal lamina-like structure, capacity to express αSMA, vimentin and laminin) were demonstrated in both primary and secondary cultures.

Cultured cells were incubated with 35 μg/ml of 5-aza-2-deoxycitidine (Sigma) for hypomethylation experiments or 10 ng/ml of murine recombinant TGF-β1 (Invitrogen) or murine recombinant PDGF (Sigma) for growth factor stimulation experiments.

Xenograft Studies in SCID Mice

All mice studies and breeding were carried out under the approval of IACUC of Columbia University. Six to 8-week-old SCID mice were used for subcutaneous injection with a mixture of tumor cells and either RFP+, RFP−, or RFP+/− αSMA-MSCs (1×10^5), or GFP-labeled BM-derived MFs (1×10^5) isolated from the stomach. Human gastric cancer cell lines MKN45 and AGS or the mouse Lung Cancer cell line TC-1 was used. Mice were followed for 6 weeks after injection of tumor cells. TGF-β was inhibited in mice with 5 mg/kg of SB-505124 (hydrochloride hydrate; Sigma); CXCR4 was inhibited in mice with 5 mg/kg of AMD3100 (Sigma), as previously described (Azab et al., 2009).

ACCESSION NUMBERS

Microarray data were deposited on the Gene Expression Omnibus (GEO) and can be found under accession number GSE23548.

SUPPLEMENTAL INFORMATION

Supplemental Information includes Supplemental Experimental Procedures, six figures, two tables, and one movie and can be found with this article online at doi:10.1016/j.ccr.2011.01.020.

ACKNOWLEDGMENTS

We would like to thank D. Brenner and S. Magness for the generous gift of αSMA-RFP and collagen-α1-GFP mice, H. Nakagawa for instructing in organotypic culture, P. Good for excellent technical assistance, A. Whelan and J. DeGrazia for managing the mouse colony, R. Chen for help with IHC, K. Novak for critical reading and editing of the manuscript, and all members of the T.C.W. laboratory for helpful comments and discussion. T.C.W. is supported by National Institutes of Health grants 1U54CA126513, RO1CA093405, and R01CA120979. M.Q. is supported by a grant from the Mildred-Scheel-Stiftung, Deutsche Krebshilfe, Germany. W.S. is supported by the Japan Society for the Promotion of Science 2009. S.T. is supported NIH grant R21CA149865.

Received: November 20, 2009
Revised: July 23, 2010
Accepted: January 10, 2011
Published: February 14, 2011

REFERENCES

Allinen, M., Beroukhim, R., Cai, L., Brennan, C., Lahti-Domenici, J., Huang, H., Porter, D., Hu, M., Chin, L., Richardson, A., et al. (2004). Molecular characterization of the tumor microenvironment in breast cancer. Cancer Cell *6*, 17–32.

Azab, A.K., Runnels, J.M., Pitsillides, C., Moreau, A.S., Azab, F., Leleu, X., Jia, X., Wright, R., Ospina, B., Carlson, A.L., et al. (2009). CXCR4 inhibitor AMD3100 disrupts the interaction of multiple myeloma cells with the bone marrow microenvironment and enhances their sensitivity to therapy. Blood *113*, 4341–4351.

Brabletz, S., Schmalhofer, O., and Brabletz, T. (2009). Gastrointestinal stem cells in development and cancer. J. Pathol. *217*, 307–317.

Coussens, L.M., and Werb, Z. (2002). Inflammation and cancer. Nature *420*, 860–867.

Direkze, N.C., Forbes, S.J., Brittan, M., Hunt, T., Jeffery, R., Preston, S.L., Poulsom, R., Hodivala-Dilke, K., Alison, M.R., and Wright, N.A. (2003). Multiple organ engraftment by bone-marrow-derived myofibroblasts and fibroblasts in bone-marrow-transplanted mice. Stem Cells *21*, 514–520.

contribute to the normal stem cell niche in the BM. In their niche, MSCs express both Gremlin-1 and SDF-1. TGF-β can induce the differentiation of MSCs into MFs through an SDF1α-dependent pathway that involves DNA hypomethylation. MFs express BMP4, which seems to induce Gremlin-1 in MSCs; BMP4 and Wnt5a likely induce DKK1 or Shh in the normal, heterogeneous population of MSCs. With cancer progression, the number of CAFs increases markedly in the BM niche and blood. These BM niche cells are expanded in a TGF-β-dependent matter and are recruited through CXCR4/SDF1α signaling together with Gremlin-1-expressing MSCs to incipient tumors where they now appear as CAFs.

Direkze, N.C., Hodivala-Dilke, K., Jeffery, R., Hunt, T., Poulsom, R., Oukrif, D., Alison, M.R., and Wright, N.A. (2004). Bone marrow contribution to tumor-associated myofibroblasts and fibroblasts. Cancer Res. *64*, 8492–8495.

Erez, N., Truitt, M., Olson, P., and Hanahan, D. (2010). Cancer-associated fibroblasts are activated in incipient neoplasia to orchestrate tumor-promoting inflammation in an NF-kappaB-dependent manner. Cancer Cell *17*, 135–147.

Forbes, S.J., Russo, F.P., Rey, V., Burra, P., Rugge, M., Wright, N.A., and Alison, M.R. (2004). A significant proportion of myofibroblasts are of bone marrow origin in human liver fibrosis. Gastroenterology *126*, 955–963.

Grivennikov, S., Karin, E., Terzic, J., Mucida, D., Yu, G.Y., Vallabhapurapu, S., Scheller, J., Rose-John, S., Cheroutre, H., Eckmann, L., and Karin, M. (2009). IL-6 and Stat3 are required for survival of intestinal epithelial cells and development of colitis-associated cancer. Cancer Cell *15*, 103–113.

Guo, X., Oshima, H., Kitmura, T., Taketo, M.M., and Oshima, M. (2008). Stromal fibroblasts activated by tumor cells promote angiogenesis in mouse gastric cancer. J. Biol. Chem. *283*, 19864–19871.

Hayward, S.W., Wang, Y., Cao, M., Hom, Y.K., Zhang, B., Grossfeld, G.D., Sudilovsky, D., and Cunha, G.R. (2001). Malignant transformation in a nontumorigenic human prostatic epithelial cell line. Cancer Res. *61*, 8135–8142.

Houghton, J., and Wang, T.C. (2005). *Helicobacter pylori* and gastric cancer: a new paradigm for inflammation-associated epithelial cancers. Gastroenterology *128*, 1567–1578.

Houghton, J., Stoicov, C., Nomura, S., Rogers, A.B., Carlson, J., Li, H., Cai, X., Fox, J.G., Goldenring, J.R., and Wang, T.C. (2004). Gastric cancer originating from bone marrow-derived cells. Science *306*, 1568–1571.

Ishii, G., Sangai, T., Oda, T., Aoyagi, Y., Hasebe, T., Kanomata, N., Endoh, Y., Okumura, C., Okuhara, Y., Magae, J., et al. (2003). Bone-marrow-derived myofibroblasts contribute to the cancer-induced stromal reaction. Biochem. Biophys. Res. Commun. *309*, 232–240.

Izadpanah, R., Kaushal, D., Kriedt, C., Tsien, F., Patel, B., Dufour, J., and Bunnell, B.A. (2008). Long-term in vitro expansion alters the biology of adult mesenchymal stem cells. Cancer Res. *68*, 4229–4238.

Jiang, L., Gonda, T.A., Gamble, M.V., Salas, M., Seshan, V., Tu, S., Twaddell, W.S., Hegyi, P., Lazar, G., Steele, I., et al. (2008). Global hypomethylation of genomic DNA in cancer-associated myofibroblasts. Cancer Res. *68*, 9900–9908.

Karnoub, A.E., Dash, A.B., Vo, A.P., Sullivan, A., Brooks, M.W., Bell, G.W., Richardson, A.L., Polyak, K., Tubo, R., and Weinberg, R.A. (2007). Mesenchymal stem cells within tumour stroma promote breast cancer metastasis. Nature *449*, 557–563.

Li, L., and Neaves, W.B. (2006). Normal stem cells and cancer stem cells: the niche matters. Cancer Res. *66*, 4553–4557.

Lo Celso, C., Fleming, H.E., Wu, J.W., Zhao, C.X., Miake-Lye, S., Fujisaki, J., Cote, D., Rowe, D.W., Lin, C.P., and Scadden, D.T. (2009). Live-animal tracking of individual haematopoietic stem/progenitor cells in their niche. Nature *457*, 92–96.

Maeshima, A.M., Niki, T., Maeshima, A., Yamada, T., Kondo, H., and Matsuno, Y. (2002). Modified scar grade: a prognostic indicator in small peripheral lung adenocarcinoma. Cancer *95*, 2546–2554.

Magness, S.T., Bataller, R., Yang, L., and Brenner, D.A. (2004). A dual reporter gene transgenic mouse demonstrates heterogeneity in hepatic fibrogenic cell populations. Hepatology *40*, 1151–1159.

Mathur, D., Bost, A., Driver, I., and Ohlstein, B. (2010). A transient niche regulates the specification of Drosophila intestinal stem cells. Science *327*, 210–213.

McKaig, B.C., Makh, S.S., Hawkey, C.J., Podolsky, D.K., and Mahida, Y.R. (1999). Normal human colonic subepithelial myofibroblasts enhance epithelial migration (restitution) via TGF-beta3. Am. J. Physiol. *276*, G1087–G1093.

Mendez-Ferrer, S., Michurina, T.V., Ferraro, F., Mazloom, A.R., Macarthur, B.D., Lira, S.A., Scadden, D.T., Ma'ayan, A., Enikolopov, G.N., and Frenette, P.S. (2010). Mesenchymal and haematopoietic stem cells form a unique bone marrow niche. Nature *466*, 829–834.

Mishra, P.J., Humeniuk, R., Medina, D.J., Alexe, G., Mesirov, J.P., Ganesan, S., Glod, J.W., and Banerjee, D. (2008). Carcinoma-associated fibroblast-like differentiation of human mesenchymal stem cells. Cancer Res. *68*, 4331–4339.

Morrison, S.J., and Kimble, J. (2006). Asymmetric and symmetric stem-cell divisions in development and cancer. Nature *441*, 1068–1074.

Okawa, T., Michaylira, C.Z., Kalabis, J., Stairs, D.B., Nakagawa, H., Andl, C.D., Johnstone, C.N., Klein-Szanto, A.J., El-Deiry, W.S., Cukierman, E., et al. (2007). The functional interplay between EGFR overexpression, hTERT activation, and p53 mutation in esophageal epithelial cells with activation of stromal fibroblasts induces tumor development, invasion, and differentiation. Genes Dev. *21*, 2788–2803.

Orimo, A., Gupta, P.B., Sgroi, D.C., Arenzana-Seisdedos, F., Delaunay, T., Naeem, R., Carey, V.J., Richardson, A.L., and Weinberg, R.A. (2005). Stromal fibroblasts present in invasive human breast carcinomas promote tumor growth and angiogenesis through elevated SDF-1/CXCL12 secretion. Cell *121*, 335–348.

Pera, M.F., Andrade, J., Houssami, S., Reubinoff, B., Trounson, A., Stanley, E.G., Ward-van Oostwaard, D., and Mummery, C. (2004). Regulation of human embryonic stem cell differentiation by BMP-2 and its antagonist noggin. J. Cell Sci. *117*, 1269–1280.

Pittenger, M.F., Mackay, A.M., Beck, S.C., Jaiswal, R.K., Douglas, R., Mosca, J.D., Moorman, M.A., Simonetti, D.W., Craig, S., and Marshak, D.R. (1999). Multilineage potential of adult human mesenchymal stem cells. Science *284*, 143–147.

Simmons, P.J., Przepiorka, D., Thomas, E.D., and Torok-Storb, B. (1987). Host origin of marrow stromal cells following allogeneic bone marrow transplantation. Nature *328*, 429–432.

Sneddon, J.B., Zhen, H.H., Montgomery, K., van de Rijn, M., Tward, A.D., West, R., Gladstone, H., Chang, H.Y., Morganroth, G.S., Oro, A.E., and Brown, P.O. (2006). Bone morphogenetic protein antagonist gremlin 1 is widely expressed by cancer-associated stromal cells and can promote tumor cell proliferation. Proc. Natl. Acad. Sci. USA *103*, 14842–14847.

Snippert, H.J., van der Flier, L.G., Sato, T., van Es, J.H., van den Born, M., Kroon-Veenboer, C., Barker, N., Klein, A.M., van Rheenen, J., Simons, B.D., and Clevers, H. (2010). Intestinal crypt homeostasis results from neutral competition between symmetrically dividing Lgr5 stem cells. Cell *143*, 134–144.

Stappenbeck, T.S., and Miyoshi, H. (2009). The role of stromal stem cells in tissue regeneration and wound repair. Science *324*, 1666–1669.

Tomita, H., Takaishi, S., Menheniott, T.R., Yang, X., Shibata, W., Jin, G., Betz, K., Kawakami, K., Minamoto, T., Tomasetto, C., et al. (2010). Inhibition of gastric carcinogenesis by the hormone, gastrin, is mediated by suppression of TFF1 epigenetic silencing. Gastroenterology, in press. Published online November 25, 2010. 10.1053/j.gastro.2010.11.037.

Tu, S., Bhagat, G., Cui, G., Takaishi, S., Kurt-Jones, E.A., Rickman, B., Betz, K.S., Penz-Oesterreicher, M., Bjorkdahl, O., Fox, J.G., and Wang, T.C. (2008). Overexpression of interleukin-1beta induces gastric inflammation and cancer and mobilizes myeloid-derived suppressor cells in mice. Cancer Cell *14*, 408–419.

Vermeulen, L., De Sousa, E.M.F., van der Heijden, M., Cameron, K., de Jong, J.H., Borovski, T., Tuynman, J.B., Todaro, M., Merz, C., Rodermond, H., et al. (2010). Wnt activity defines colon cancer stem cells and is regulated by the microenvironment. Nat. Cell Biol. *12*, 468–476.

Wang, S.S., Asfaha, S., Okumura, T., Betz, K.S., Muthupalani, S., Rogers, A.B., Tu, S., Takaishi, S., Jin, G., Yang, X., et al. (2009). Fibroblastic colony-forming unit bone marrow cells delay progression to gastric dysplasia in a *Helicobacter* model of gastric tumorigenesis. Stem Cells *27*, 2301–2311.

Wicha, M.S., Liu, S., and Dontu, G. (2006). Cancer stem cells: an old idea—a paradigm shift. Cancer Res. *66*, 1883–1890.

Worthley, D.L., Ruszkiewicz, A., Davies, R., Moore, S., Nivison-Smith, I., Bik To, L., Browett, P., Western, R., Durrant, S., So, J., et al. (2009). Human gastrointestinal neoplasia-associated myofibroblasts can develop from bone marrow-derived cells following allogeneic stem cell transplantation. Stem Cells *27*, 1463–1468.

Yokota, T., Kawakami, Y., Nagai, Y., Ma, J.X., Tsai, J.Y., Kincade, P.W., and Sato, S. (2006). Bone marrow lacks a transplantable progenitor for smooth muscle type alpha-actin-expressing cells. Stem Cells *24*, 13–22.

Zhang, J., and Li, L. (2005). BMP signaling and stem cell regulation. Dev. Biol. *284*, 1–11.